White Paper:
Modeling heat transfer in a W+C powder bed in a pusher furnace

By Peter Witting, Harper International
T.J Jewett, Global Tungsten & Powders

ABSTRACT

The nature of the WC produced in pusher furnaces is influenced by numerous variables, including the temperature profile in the furnace, boat geometry, powder bed depth and density, and the thermal diffusivity of the powder bed. The current investigation has been undertaken to assist in the design of W carburization furnaces with the objective of obtaining uniform heating of the powder bed. The thermal diffusivity of the powder bed was determined from heating experiments conducted with a mixture of W powder (FSSS 20 µm) and carbon in an Inconel 601 capsule, with multiple thermocouples recording the powder bed temperature. The capsule heating was modelled using the FEA technique and thermal diffusivity as a function of temperature was determined by optimizing the fit of the model to the experiments. The effect of the powder bed density was also studied by running experiments by varying the powder bed compaction. The model was then applied to real carburization furnace configurations. Design parameters studied included: muffle geometry, boat size and aspect ratio and single vs. stacked boat designs.

INTRODUCTION

In pusher-type furnaces the product carrier is introduced into the furnace by a mechanical pusher mechanism. The product carrier can consist of a cylindrical boat in the case of a tubular pusher system, or a rectangular boat with a lid in the case of a system with a flat hearth plate. The product boats are sequentially pushed into the furnace, moving the train of boats in and out of the furnace system. Pusher systems are designed for processes requiring precise control of both the temperature and atmosphere. They are ideal for processes with longer residence times that require exact control of the product heat up rate (temperature profile) and limited gas/solid reaction.

Proper design of a pusher furnace for a given process requires careful thermal analysis of the furnace and the product. The thermal conductivity of the product is needed to calculate the time required to reach a uniform product temperature under different furnace configurations. Unfortunately, in the case of powders, data on thermal conductivity is rarely available.

The goal of this study was to improve the predictive capability of furnace thermal modeling through the experimental measurements of time-to-temperature for various tungsten and carbon mixtures under a variety of conditions. This data was used to calculate the thermal diffusivity of the powder as a function of temperature. A model for the thermal conductivity was then adjusted to best fit the experiments. Finally, the model was utilized to calculate conductivity of different powders under various processing conditions.

Model for the thermal conductivity of the powder bed

We use the thermal conductivity model presented by Sih *et al* in [1, 2]. Some of the assumptions are briefly explained below; a more detailed review of the model can be found in [3]. The tungsten and carbon particles are assumed to be spherical. Uniform particle size is also assumed. In general, for small particle size, the contribution of radiation to the effective thermal conductivity is small, in comparison to the contribution of conduction through the solid particles and convection in the gas phase. The radiation component becomes a significant contributor as the temperature and particle size increase. For the analysis presented in this paper, the radiation component was included in all cases. Radiation is a significant contributor in the nitrogen atmosphere cases. Conductivity of the powder is given by

$$\frac{k}{k_g} = \left(1 - \sqrt{1-\varepsilon}\right)\left(1 + \frac{\varepsilon k_R}{k_g}\right) + \sqrt{1-\varepsilon}\left[\frac{2}{1 - \frac{k_g}{k_s}}\left(\frac{1}{\left(1 - \frac{k_g}{k_s}\right)} \ln \frac{k_g}{k_s} - 1\right) + \frac{k_R}{k_g}\right]$$

Free Fluid Core Heat Transfer

Where

$k_R = 4F d_p \sigma T^3$ ($\mathrm{k_R}$ conductivity by thermal radiation)

F = View Factor

T = Absolute temperature of the powder bed

σ = stefan − boltzmann constant

d_p = Particle diameter

k = Effective thermal conductivity of the powder bed

k_g = Thermal conductivity of the gas phase

k_s = Thermal conductivity of the solid phase

ε = Porosity of the powder bed

EXPERIMENTAL PROCEDURES

Tungsten metal powder and carbon powder, N990, were blended to a 6.10wt%C target. The milling took place in a 330 mm ball mill loaded with 25 kg of the sample powder and 45 kg of 6 mm diameter WC-Co milling media. The powder was processed on a roll mill for 2 hours at 60 Hz. The powder mixture was loaded into an alloy cylindrical canister with a five foot extension pipe 15.9 mm in diameter. The extension pipe housed two thermocouples and carried the process gas to the canister. Five Inconel sheathed K-type thermocouples were inserted into the bed material. A thermocouple of the same type was placed on the outside of the canister. Nitrogen flowed on the outside of the canister for each test and the furnace was kept at positive pressure. Nitrogen or helium was used as the process gas. A welding torch was used to apply a layer of carbon soot to the outside of the vessel to assist with heat transfer. A schematic of the test apparatus is shown in Figure 1.

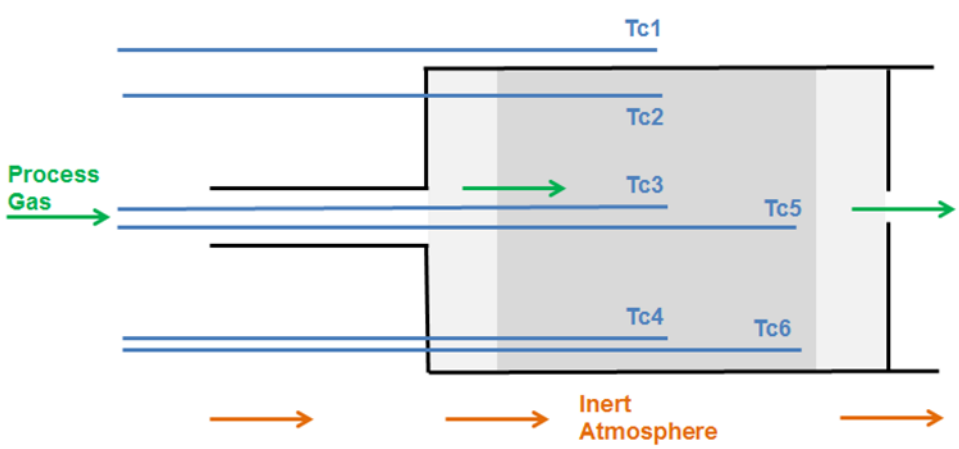

Figure 1: Design of the powder canister used in the powder heating tests.

Powder heating experiments

Each test required setup and furnace heat up prior to starting. The setup began by weighing the canister and adding material to a maximum height of three inches from the top of the open end of the canister. If packed material was required, additional material was added to reach the desired height within the canister. Insulation was placed on top of the exposed material and then a metal end cap. The end cap was tack welded at four equally spaced locations around the circumference. The canister was then threaded on the extension pipe. The thermocouples were then inserted into the bed of the material through openings in the canister and insulation. Process gas was connected and the vessel purged with process gas for a minimum of 15 minutes. During this time, the furnace was also purged with nitrogen.

The furnace was heated to the same conditions for each test. Zones one and three were both heated to 1,050°C. The hot zone where the canister was placed, zone two, was heated to 1,150°C. After the furnace zones reached temperature and both the tube and canister had been purged, the canister inserted into zone 2 to start the test. The test configuration showing the position of the capsule within the furnace is shown in Figure 2.

Temperatures were recorded using a DAQ data logging program. Once all the thermocouple temperatures reached equilibrium with the furnace hot zone temperature, the canister was pulled back to the cool zone. The canister remained in the cooling zone under purge until the material bed temperatures fell below 400°C to prevent oxidation. It was then removed from the furnace and cooled to below 100°C before handling.

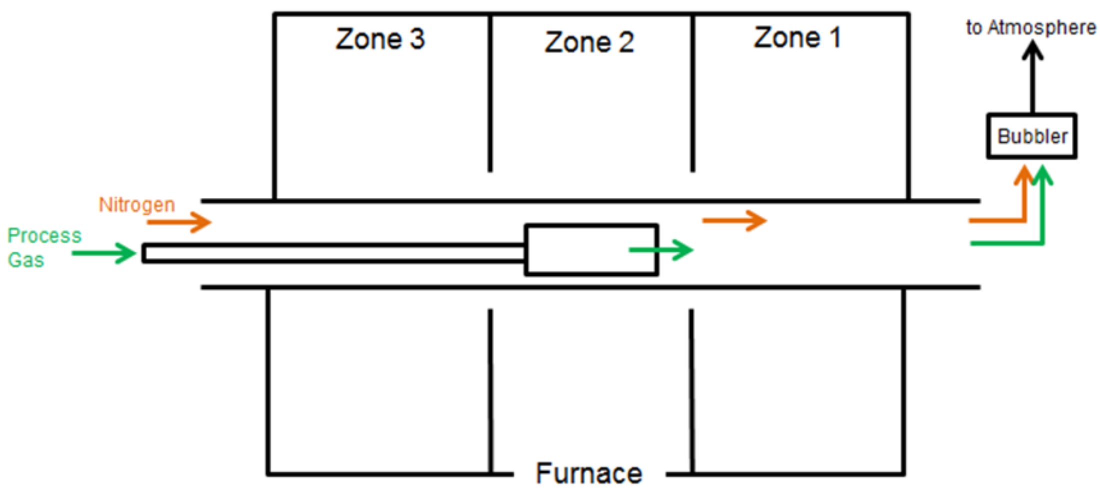

Figure 2: Furnace test set up

Conductivity of the tungsten + C powder bed

The thermal conductivity of the powder bed was calculated in two ways:

1. Using the Sih & Barlow model (Equation1.)
2. Modelling the canister heating tests and adjusting the thermal diffusivity $\alpha(T)$ to obtain the best fit between the model and the experiments for the temperature history at the center of the canister. Then determining the conductivity from:

$$k(T) = \alpha(T)\rho C_p \qquad (2)$$

Where ρ and C_p are the density and the specific heat of the powder bed, respectively.

The values of thermal conductivity calculated by each method were compared to assess the accuracy of the Sih & Barlow model.

For the experiments two types of tungsten plus carbon samples where tested at various packing densities and processing atmospheres. The tests are summarized in Table I. The density of the powder bed was recorded prior to each test. The specific heat was calculated by the rule of mixtures (Table II).

Table I: Test matrix

Test #	Temperature °C	Material	Average Particle size LM-FSSS µm	Fill Type	Density g/cm^3	Process Gas
1	1,150	W75	15.2	Semi-loose	5.1	Helium
2	1,150	W75	15.2	Tamped	6.2	Helium
3	1,150	W37	2.5	3.6	Nitrogen	Helium
4	1,150	W37	2.5	4.7	Nitrogen	
5	1,150	W75	15.2	Vibrated		

Table II: Specific heat of W+C powder

Temperature °C	Cp of W+C J/kg°C
0	170
100	204
500	245
1000	267
1500	285
2000	302

Modelling the powder heating experiments

The canister heating tests were modeled using an axisymmetric finite element method (FEM) model to solve the heat conduction equation numerically. For this model the process gas flow was neglected as a small heat sink on the system. The boundary conditions for the canister were modelled by applying the temperature history measured by the thermocouple TC1 that was located on the external surface of the canister.

The calculated temperature histories at each thermocouple location are plotted in Figure 3. The thermal diffusivity of the powder bed, $\alpha(T)$, was adjusted to obtain the best fit between the model and the experiments for the temperature history at the center of the canister.

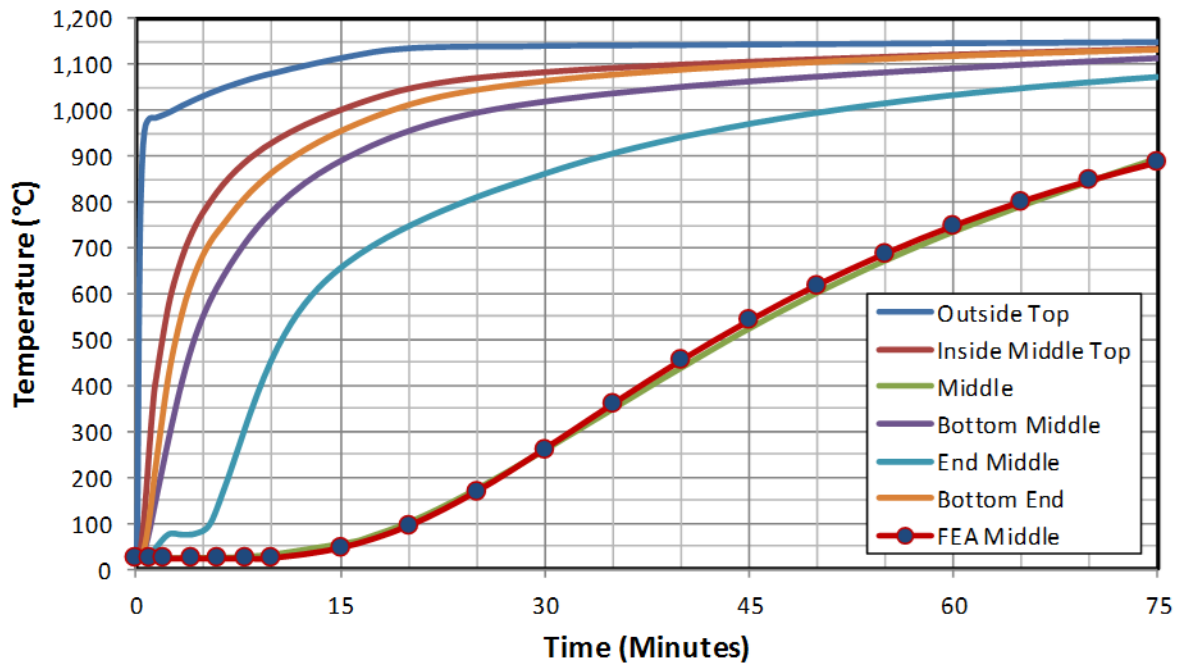

Figure 3: Test 1 Time Temperature Curves: SC75, Semi Loose 5.1 g/cc, Helium

Measured effect of powder bed density, grain size and cover gas on conductivity

Figure 4 presents the average thermal conductivities calculated for the different tests. In general, the conductivity increases with density. The two different powder grain size tested seems to have only a minor effect on the conductivity. Thermal conductivity under N_2 gas is lower than the conductivity under He gas, however, this is confounded by the fact that all the tests under He used higher powder bed densities.

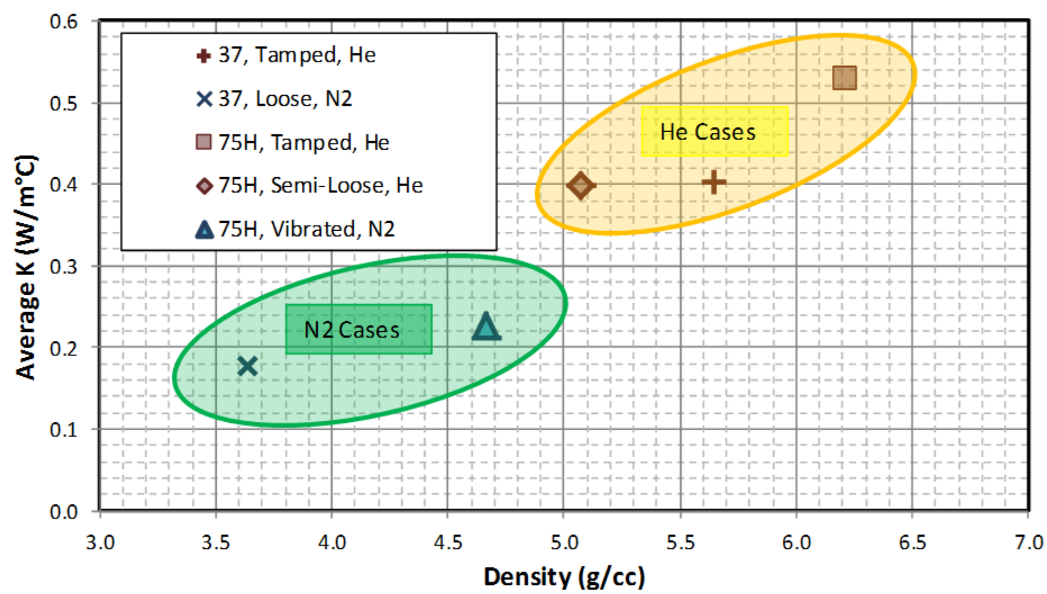

Figure 4: Average thermal conductivity calculated by modelling the powder heating tests.

Assessment of the Accuracy of the Thermal Conductivity Predictions

Given the wide range of values for the conductivity of carbon reported in the literature [4, 5], we used high and low bounding values to form a range for comparison. The thermal conductivities of tungsten were taken from [6]. There is also some uncertainty with the conductivity of the W particles because the particles may not be fully dense, which would affect their conductivity. The thermal conductivity as a function of temperature used in the analysis of the W and Carbon particles is listed in Table III. The large range in the thermal conductivity of the carbon leads to a “high” and “low” range in average particle thermal conductivity.

The conductivity calculated with the Sigh and Barlow model is compared to the values calculated from the FEM modelling of the canister heating tests 1 and 5 in Figures 5 and 6. The “high” and “low” labels in the plots correspond to the use of the high and low values of k for carbon.

Table III: Summary of temperature dependent thermal conductivity of particles

Temperature	Carbon - Low	Graphite (Carbon "high" Value)	Tungsten	Average of Carbon and W	Average of Graphite and W
°C	W/m°C	W/m°C	W/m°C	W/m°C	W/m°C
100	3	110	160	81	135
500	6	64	126	66	95
1000	8	40	112	60	76
1500	8	33	104	56	69

Test 1 was conducted and He gas. In this and in the other tests conducted under He cover gas, the model over-predicts the thermal conductivity of the bed (Figure 5.) In comparing the data to a model for the case of an N_2 cover gas, the model under predicted the thermal conductivity of the bed. Using a simple mixing rule, the data matches the predicted thermal conductivity if the N_2 % is increased from zero to between 40 and 65%. This reduces the effect of the highly conductive He on the model and lowers the prediction. It is also possible that during the test N_2 was not fully removed from the powder bed, so a mixture of He and N_2 may have existed in the bed of material.

Figure 6 presents results for test 5, where N_2 was used as the process gas. Here, and in test 6 (not shown), the best agreement between the model and the experiments is obtained with the “low” prediction of thermal conductivity. The data are between the low and high predicted values but closer to the low prediction.

Based on these results, the Sih & Barlow model was used for further calculations with the following adjustments:

1. Always use the low value for C conductivity
2. For cases under He, use the model with an atmosphere composition of 60% N_2 and 40%.

With these adjustments and equation 2, the thermal diffusivity $\alpha(T)$ was calculated for the different powder bed compositions and densities. The densities selected are based on the densities in the lab for tamped (higher bulk density) and vibrated (lower bulk density) processing. The calculated $\alpha(T)$ values are summarized in Table IV.

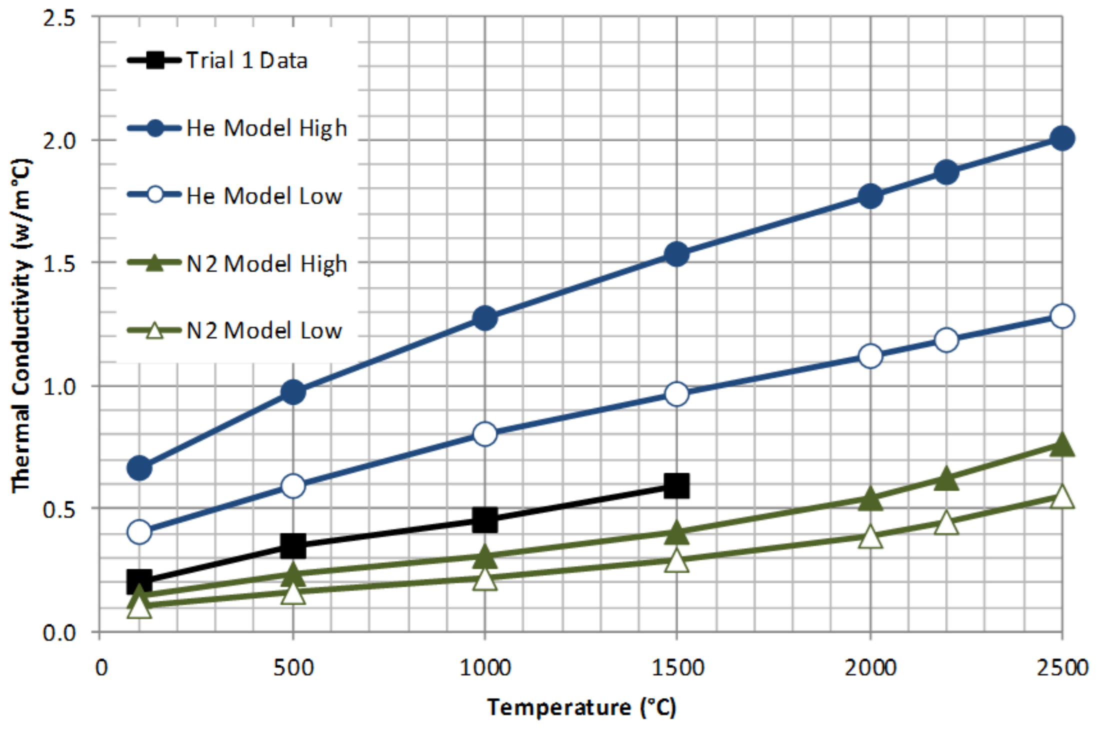

Figure 5: Comparison of Trial 1, W75 in He with Predicted Thermal Conductivity

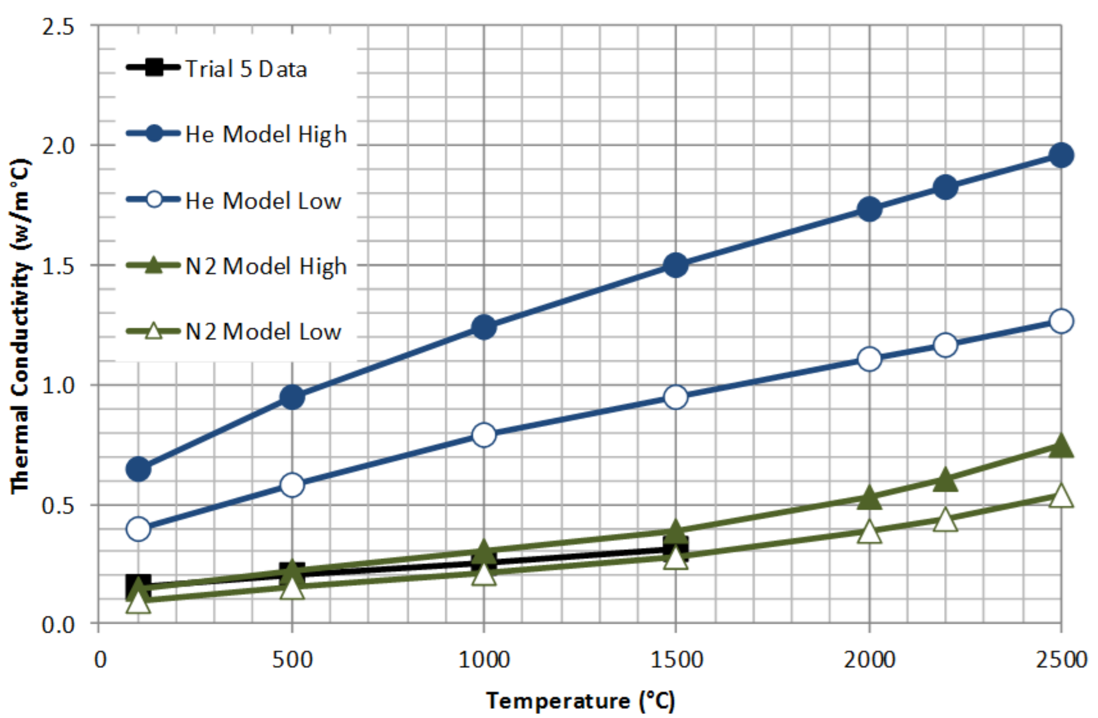

Figure 6: Comparison of Trial 5, W75 in N_2 with Predicted Thermal Conductivity

Table IV: Summary of thermal diffusivities calculated according to the adjusted Sih & Barlow model

Material	W37	W37	W37	W37	W75	W75	W75	W75
Atmp	N2	He	N2	He	N2	He	N2	He
Density	3.6 g/cc	3.6 g/cc	5.6 g/cc	5.6 g/cc	4.7 g/cc	4.7 g/cc	6.2 g/cc	6.2 g/cc
Temp (° C)	α (mm²/ sec)	α (mm²/ sec)	α (mm²/ sec)	α (mm²/ sec)	α (mm²/ sec)	α (mm²/ sec)	α (mm²/ sec)	α (mm²/ sec)
100	0.123	0.320	0.092	0.235	0.103	0.265	0.086	0.219
500	0.161	0.405	0.120	0.294	0.136	0.335	0.113	0.275
1000	0.199	0.508	0.147	0.366	0.172	0.422	0.142	0.345
1500	0.235	0.634	0.173	0.452	0.211	0.532	0.173	0.431
2000	0.290	0.835	0.212	0.586	0.271	0.705	0.221	0.565
2200	0.319	0.939	0.232	0.654	0.303	0.793	0.246	0.632
2500	0.372	1.121	0.269	0.771	0.360	0.947	0.291	0.749

1D Bed Time to Temperature Predictions

A FEA analysis was performed for a 1 dimensional rectangular bed of various bed depths. This is an extension to the classical problem with an exact solution of a plane wall with convection and constant convection coefficients, diffusivities, etc. In this case the 1 dimensional problem is the same except all of the variables (radiation boundary condition, thermal conductivity, and specific heat) are temperature dependent so an exact solution is not available. The radiation boundary condition is placed on the edge of the rectangular bed and the FEA was run with the appropriate material properties. The model uses ½ of the overall thickness with the boundary condition applied only to one edge of the bed. The model assumes symmetry around the center of the bed. A model of the time temperature relation for processing at 2200°C was generated for this pusher configuration operating under a N_2 process gas is presented in Figure 7, with the various lines indicating the full bed depth.

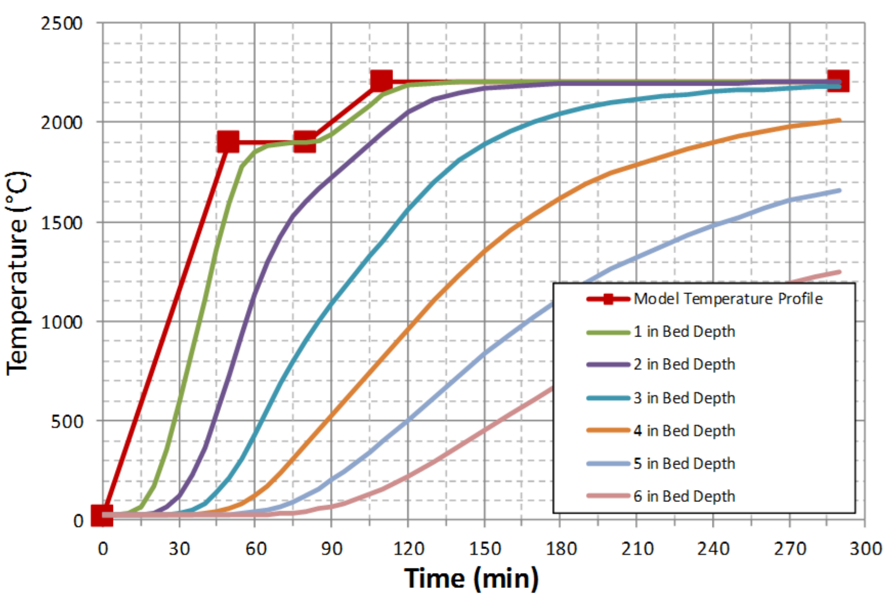

Figure 7: Time Temperate of SC75 Material, N_2, 4.7 g/cc

Modelling Various Pusher Furnace Configurations

Several models (Figure 8) were prepared to investigate the effect of powder bed depth and boat and muffle geometry. The models are 2-dimensional thermal models considering radiation and conduction heat transfer. Convection heat transfer is neglected in these models due to its small contribution in heat transfer at the applied temperatures. A graphite muffle has a time dependent radiation boundary conditions on the outside surface which represents a time-temperature profile of a pusher furnace. Since the graphite muffle is stationary and the graphite boat and product move through the muffle, only the graphite boat and product absorb energy. To mimic this condition in a 2-dimensional model the graphite material properties of the muffle are modified by reducing the specific heat and density values 3 orders of magnitude lower than the actual values. The thermal conductivity remains the actual value. The lowering of the specific heat and density results in the muffle being at queasy steady state and absorbing negligible heat content. This method of modified properties allows a 2-demensional model to capture the effective heat transfer of a moving boat inside a stationary muffle without the computational penalty of a 3-dimensional model. The graphite boat and product use the estimated specific heat and density. N_2 was used as the process gas, with the processing temperature set to 2200°C.

The calculated temperature profiles are summarized in Figure 8. One result is immediately clear, the deeper the bed depth, the greater the temperature gradient between the outside of the graphite vessel and the core of the powder bed. Separating the vessel into a stacked unit reduces the contiguous powder bed, and helps reduces the gradient. However, a significant temperature spread is still observed partly due to the additional graphite mass. The wide shallow bed results in a reduction in time to temperature (Figure 7) of the bed material compared to the lower aspect ratio shapes.

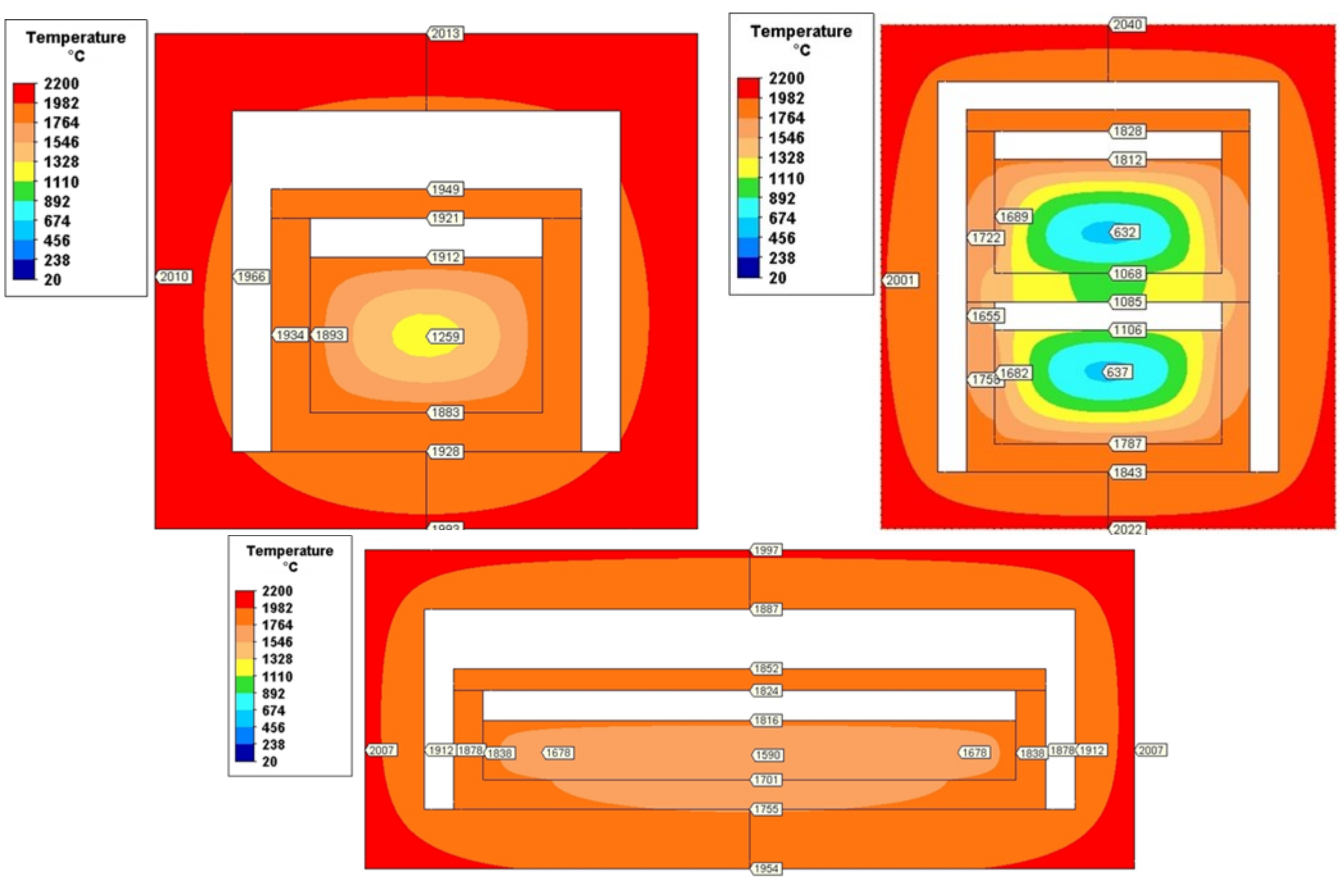

Figure 8: Powder bed modelling for various boat and muffle geometries

Conclusions

The Sih & Barlow model for the thermal conductivity of a powder was applied to the calculation of the conductivity of a WC + C powder bed. The accuracy of the model was assessed through the modelling of a series of experimnets that involved heating of a powder in a canister. Best results were obtained by introducing two ajustments to the model:1) of the reported values for the conductivity of C, used the low values of thermal conductivity reported in Table III, and 2) when working with He atmosphere, modeled the atmosphere as a mixture of 60% N_2 and 40% H_2.

The thermal conductivity from the Sih& Barlow model was incorporated in the modelling of the carburization of W in a pusher furnace. Several powder bed depths and geometric configurations were analyzed and the resulting temperature fields were reported.

The examples demonstrate that modelling is a very valuable tool that can guide the optimization of powder bed, boat and furnace geometry. Of course, the final design must account for other practical factors like material handling, furnace construction and throughput.

Future refinements to the model will include accounting for the heat associated with the carburization reaction. Another aspect that could be addressed is the changes associated with the progress of the carburization reaction. As the reaction progresses, the nature of the powder bed changes, the C particles are consumed, the W is converted to WC, the particle size changes and the density of the bed also changes. All these factors have an impact on the effective conductivity.

References

1. Sih, S. S. & Barlow, J. W., 1994. Measurement and prediction of the Thermal Conductivity of Powders at High Temperatures. Austin, s.n., pp. 321-329.
2. Sih, S. S. & Barlow, J. W., 1995. The Predictions of Thermal Conductivity of Powders. Austin, s.n., pp. 397-401.
3. Witting, P. & Dover, B., 2014. Analysis of the Heating of Powders in a 'Pusher' Furnace, in Proceedings of the PM2014 World Congress on Powder Metallurgy and Particulate Materials, Orlando, 2014. MPIF, New Jersey, USA.
4. Craig W. Ohlhorst, W. L. V. P. O. R. a. H.-T. T., 1997. Thermal Conductivity Database of Various Structural Carbon-Carbon Composite Materials, Hampton: Langley Research Center.
5. Page, D. J., 1991. The Industrial Graphite Engineering Handbook. Danbury: UCAR Carbon Technology Corporation.
6. Lassner, E. & Schubert, W.-D., 1999. Tungsten. New York: Plenum Publishers